Direct Observation of Dynamical Bifurcation between Two Driven Oscillation States of a Josephson Junction

I. Siddiqi, R. Vijay, F. Pierre, C. M. Wilson, L. Frunzio, M. Metcalfe, C. Rigetti, R. J. Schoelkopf, and M. H. Devoret
Departments of Applied Physics and Physics, Yale University, New Haven, Connecticut 06520-8284, USA

D. Vion and D. Esteve
Service de Physique de l'Etat Condensé, CEA-Saclay, F-91191 Gif-sur-Yvette, France
(Received 1 October 2003; published 20 January 2005)

We performed a novel phase-sensitive microwave reflection experiment which directly probes the dynamics of the Josephson plasma resonance in both the linear and the nonlinear regime. When the junction was driven below the plasma frequency into the nonlinear regime, we observed for the first time the transition between two different dynamical states predicted for nonlinear systems. In our experiment, this transition appears as an abrupt change in the reflected signal phase at a critical excitation power. This controlled dynamical switching can form the basis of a sensitive amplifier, in particular, for the readout of superconducting qubits.

DOI: 10.1103/PhysRevLett.94.027005 PACS numbers: 85.25.Cp, 05.45.–a

As first understood by Josephson, a superconducting tunnel junction can be viewed as a nonlinear, nondissipative, electrodynamic oscillator [1]. The question we address in this Letter is whether the nonlinearity of the Josephson junction can be harnessed controllably and robustly to provide an amplification mechanism that will remain efficient in the quantum limit [2].

The tunneling of Cooper pairs manifests itself as a nonlinear inductance that shunts the linear junction self-capacitance C_J, formed by the junction electrodes and the tunnel oxide layer. The constitutive relation of the nonlinear inductor can be written as $I(t) = I_0 \sin\delta(t)$, where $I(t)$, $\delta(t) = \int_{-\infty}^{t} dt' V(t')/\varphi_0$ and $V(t)$ are the current, gauge-invariant phase difference and voltage corresponding to the inductor, respectively, while the parameter I_0 is the junction critical current. Here $\varphi_0 = \hbar/2e$ is the reduced flux quantum. For small oscillation amplitude, the frequency of oscillation is given for zero bias current by the so-called plasma frequency $\omega_P = 1/\sqrt{L_J C_J}$, where $L_J = \varphi_0/I_0$ is the effective junction inductance. As the oscillation amplitude increases, the oscillation frequency decreases, an effect which has been measured in both the classical and the quantum regime [2–6]. However, a more dramatic nonlinear effect should manifest itself if the junction is driven with an ac current $i_{\mathrm{rf}} \sin\omega t$ at a frequency ω slightly below ω_P. If the quality factor $Q = C_J \omega_P / \mathrm{Re}[Z^{-1}(\omega_P)]$ is greater than $\sqrt{3}/2\alpha$, where $Z(\omega_P)$ is the impedance of the junction electrodynamic environment and $\alpha = 1 - \omega/\omega_P$ is the detuning parameter, then the junction should transit from one dynamical oscillation state to another when i_{rf} is ramped above a critical value i_B [7]. For $i_{\mathrm{rf}} < i_B$, the oscillation state would be low amplitude and phase lagging, while for $i_{\mathrm{rf}} > i_B$, the oscillation state would be high amplitude and phase leading. This generic nonlinear phenomenon, which we refer to as "dynamical bifurcation," is reminiscent of the usual switching of a hysteretic junction from the zero-voltage state to the voltage state when the current bias exceeds the critical current I_0 [8]. However, an important distinction between dynamical bifurcation and switching is that in the former, the phase particle remains confined to only one well of the junction cosine potential $U(\delta) = -\varphi_0 I_0 \cos(\delta)$, and the time-average value of δ and $\dot{\delta}$ is always zero in each state. Note also that, unlike the critical current in switching, i_B depends both on Q and on the detuning α. In this Letter we report the first observation of a controlled dynamical bifurcation effect in a Josephson junction. As with switching, controlled dynamical bifurcation can be used for amplification [9], but with the added advantage that no energy dissipation occurs in the junction chip, a desirable feature for the readout of superconducting qubits [10].

Typical junction fabrication parameters limit the plasma frequency to the 20–100 GHz range where techniques for addressing junction dynamics are inconvenient. We have chosen to shunt the junction by a capacitive admittance to lower the plasma frequency by more than an order of magnitude and attain a frequency in the 1–2 GHz range (microwave L band). In this frequency range, a simple on-chip electrodynamic environment with minimum parasitic elements can be implemented, and the hardware for precise signal generation and processing is readily available. In our experiment, we directly measure the plasma resonance in a coherent microwave reflection measurement. Unlike previous experiments which measured only the microwave power absorption at the plasma resonance [3,4,6], we also measure the phase ϕ of the reflected microwave signal. Thus, we can detect the characteristic signature of the transition between different oscillating states of the junction—a change of oscillation phase relative to the drive. Note that the phase ϕ of the reflected signal which probes the phase of the oscillation state should not be

TABLE I. Sample parameters. $L_J = \varphi_0/I_0$ and ω_p are measured values. C and L_S are fit values to the data. Samples 1, 2, and 2a have a 100 nm thick Au underlayer, sample 3 has a 50 nm thick Nb underlayer, sample 4 has a 1 μm thick Cu underlayer, and sample 5 has a 200 nm thick Nb underlayer.

Sample	L_J (nH)	$\omega_p/2\pi$ (GHz)	C (pF)	L_S (nH)
1	0.28	1.18	39 ± 1	0.20 ± 0.02
2	0.18	1.25	30 ± 4	0.34 ± 0.04
2a	0.17	1.66	18 ± 1	0.32 ± 0.02
3	0.32	1.64	16 ± 1	0.27 ± 0.02
4	0.38	1.81	19 ± 1	0.026 ± 0.02
5	0.40	1.54	19 ± 1	0.15 ± 0.02

confused with the junction gauge-invariant phase difference δ.

In the first step of sample fabrication, a metallic underlayer—either a normal metal (Au, Cu) or a superconductor (Nb)—was deposited on a silicon substrate to form one plate of the shunting capacitor, followed by the deposition of an insulating Si_3N_4 layer. Using e-beam lithography and double-angle shadow mask evaporation, we subsequently fabricated the top capacitor plates along with a micron sized $Al/Al_2O_3/Al$ tunnel junction. The critical current of the junction was in the range $I_0 = 1$–2 μA. By varying both the dielectric layer thickness and the pad area, the capacitance C was varied between 16 and 40 pF. Sample parameters are listed in Table I.

The junction + capacitor chip is placed on a microwave circuit board and is wire bonded to the end of a coplanar strip line which is soldered to a coaxial launcher affixed to the sidewall of the copper sample box. We anchor the rf leak-tight sample box to the cold stage of a ^{3}He refrigerator with a base temperature $T = 280$ mK. The measurement setup is schematically shown in Fig. 1. Microwave excitation signals are generated by a HP 8722D vector network analyzer and coupled to the sample via the -13 dB side port of a directional coupler. The reflected microwave signal passes through the direct port of the coupler and is amplified first using a cryogenic 1.20–1.85 GHz high electron mobility transistor amplifier with noise temperature $T_N = 4$ K before returning to the network analyzer. A bias current can be applied to the junction by way of a bias tee and a passive filter network.

We locate the linear plasma resonance by sweeping the excitation frequency from 1 to 2 GHz and measuring the complex reflection coefficient $\Gamma(\omega) = (1 - \epsilon)e^{j\phi} = [Z(\omega) - Z_0]/[Z(\omega) + Z_0]$, where $Z_0 = 50$ Ω is the characteristic impedance of our transmission lines and $Z(\omega)$ is the impedance presented to the analyzer by the chip and the measurement lines. For an ideal LC resonator without intrinsic dissipation, we expect a phase shift $\phi_{\omega \gg \omega_p} - \phi_{\omega \ll \omega_p} = 2\pi$, which we verified by placing a chip capacitor and an inductive wire bond in place of the junction chip. An important aspect of our experiment is that Q is now

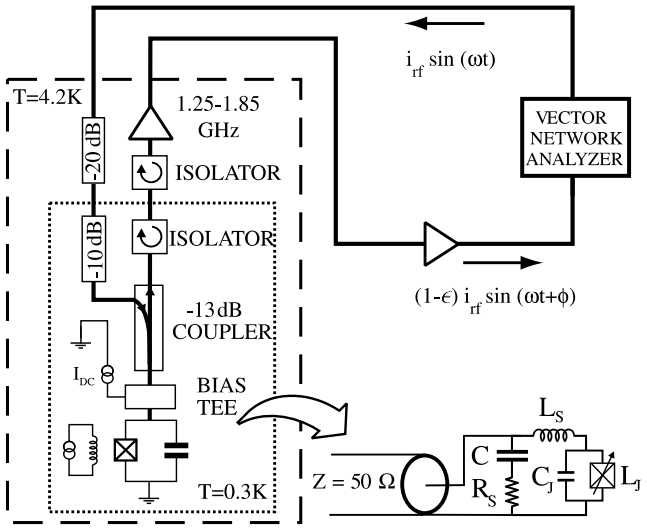

FIG. 1. Schematic of the measurement setup. Thick lines correspond to 50 Ω coaxial transmission lines. A lumped element model for the junction chip and measurement line is shown in the lower right corner.

determined by the ratio $Z_0/Z_J \sim 10$, where $Z_J = \sqrt{L_J/(C_J + C)}$ and not by the intrinsic junction losses which are negligible. An excitation power $P = i_{rf}^2 Z_0/4 \approx -120$ dBm (1 fW) corresponding to a current $i_{rf} = 9$ nA $\ll I_0$ keeps the junction in the linear regime.

In Fig. 2, we present the reflected signal phase ϕ as a function of excitation frequency for sample 5. In order to remove the linear phase evolution associated with the finite length of the measurement lines, we have subtracted from

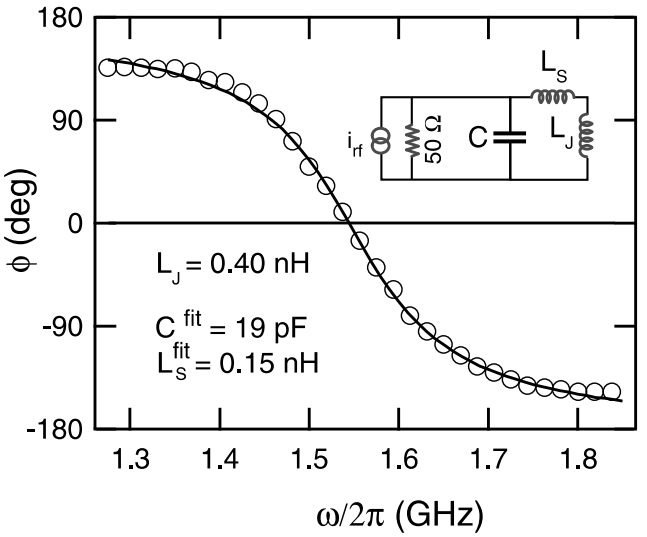

FIG. 2. Normalized reflected signal phase ϕ as a function of the excitation frequency for sample 5. The open circles are measured data for $L_J = 0.40$ nH. The solid line is calculated from the equivalent circuit model shown in the inset. Here $\epsilon = 0$ for this sample.

our measurement in the superconducting state the reflection coefficient measured with the junction in the normal state. The frequency where $\phi = 0$ thus yields the linear-regime plasma frequency. For sample 5, $\omega_p/2\pi = 1.54$ GHz.

The precise frequency and critical current dependence of the reflected signal phase of our samples can be accounted for by a three-element model for the electrodynamic environment seen by the junction. This lumped element model is shown in the lower right corner of Fig. 1. The parasitic inductance L_S and resistance R_S model the nonideality of the shunting capacitor C. They arise from the imperfect screening of currents flowing in the capacitor plates and the finite conductivity of these plates. The plasma frequency in the linear regime is determined by the total inductance $L_J + L_S$ and capacitance $C_{\text{eff}} = C_J + C \simeq C$ and is given by the following relation:

$$\left(\frac{1}{\omega_p}\right)^2 = C(L_J + L_S) = \frac{\varphi_0 C}{I_0} + CL_S.$$

We thus plot $1/\omega_p^2$ versus $1/I_0 = L_J/\varphi_0$ in Fig. 3 for samples 1, 2, 4, and 5. As the critical current is decreased by applying a magnetic field, the junction inductance increases, and the plasma frequency is reduced. For each sample, a linear fit to the data of Fig. 3 yields the values of C and L_S (see Table I). The fit values for C agree well with simple estimates made from the sample geometry. Samples 1 and 2 have nominally the same capacitance but a different critical current and hence lie approximately on the same line in Fig. 3. A total of four capacitive pads were used to make the shunting capacitor in samples 1 and 2, and after initial measurements, we scratched off two of the pads from sample 2 to obtain sample 2a, and the resulting capacitance is indeed halved. For samples with a thin underlayer (1, 2, and 3), a stray inductance in the range $L_S = 0.20$–0.34 nH is observed. For samples 4 and 5 with a significantly thicker underlayer, L_S was reduced to 0.026 and 0.15 nH, respectively. This behavior is consistent with the calculated screening properties of our thin films. To verify that the values of C and L_S were not affected by the magnetic field used to vary I_0, we varied L_J by applying a bias current [6] at zero magnetic field. The resonance data obtained by this method agree with the magnetic field data. Using L_S and C we can accurately predict the observed resonant line shape of Fig. 2, in which $R_S = 0$. For samples with a normal underlayer, we find the data are accurately fit by $R_S = 0.8\Omega$ for samples 1 and 2 and $R_S = 0.02\ \Omega$ for sample 4. Finally, we have independently verified the effect of the shunting capacitor on the plasma resonance by performing resonant activation experiments [5].

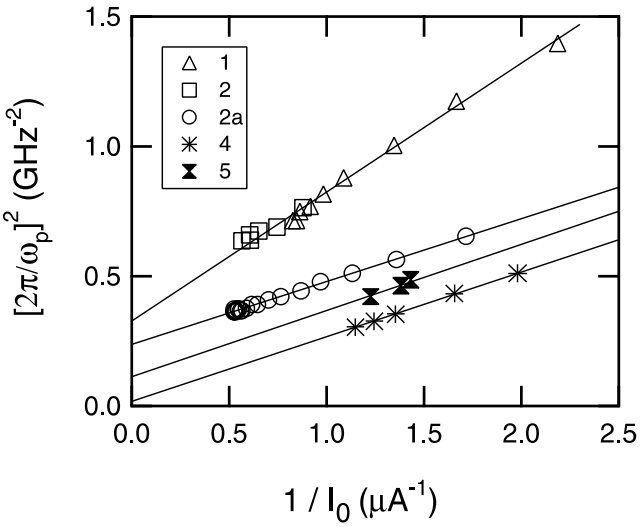

FIG. 3. Inverse square of the plasma frequency $1/\omega_p^2$ as a function of the inverse critical current $1/I_0 = L_J/\varphi_0$ for samples 1, 2, 4, and 5. Solid lines are linear fits to the data corresponding to the model of Fig. 1, with a single best fit line drawn for samples 1 and 2 which nominally differ only in I_0.

We now address our main interest: the nonlinear regime of the plasma resonance. The reflection coefficient as a function of frequency for increasing power for sample 5 is presented in the lower panel of Fig. 4 as a two dimensional color plot, in which each row is a single frequency sweep, similar to Fig. 2. For small excitation power, we recover the linear plasma resonance at 1.54 GHz, shown as a yellow line corresponding to $\phi = 0$. As the power is increased above -115 dBm, the plasma frequency decreases as is expected for a junction driven with large amplitude [5]. The boundary between the leading-phase region (green) and the lagging-phase region (red) therefore curves for high powers. This curvature has an interesting consequence: When we increase the drive power at a constant frequency slightly below the plasma frequency, the phase as a function of power undergoes an abrupt step, as predicted. For yet greater powers (> -90 dBm), we encounter a new dynamical regime (black region in Fig. 4) where δ appears to diffuse between the wells of the cosine potential. This was confirmed by the presence of an unambiguous audiofrequency ac resistance in the black region. In the lower panel of Fig. 4, we illustrate the sequence of dynamical transitions by plotting ϕ as a function of incident power at $\omega/2\pi = 1.375$ GHz. For $P < -102$ dBm, the phase is independent of power (δ oscillates in a single well in the harmonic-like, phase-leading state (A)]. For $-102 < P < -90$ dBm, the phase evolves with power and δ still remains within the same well but oscillates in the anharmonic phase-lagging state (B). Finally, for $P > -90$ dBm, the average phase of the reflected signal saturates to $-180°$, corresponding to a capacitive short circuit (C). This last value is expected if δ hops randomly between wells, the effect of which is to neutralize the Josephson inductive admittance.

The value of the current i_B for the A-B transition, which is a function of both the detuning α and power P, is in good

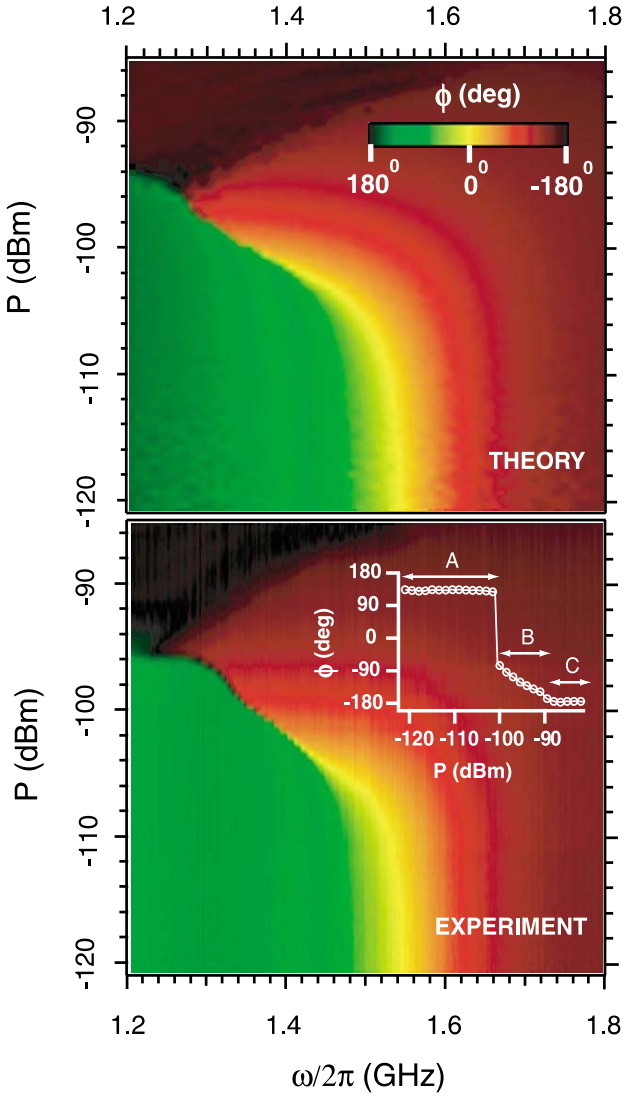

FIG. 4 (color). Normalized reflected signal phase ϕ (wrap-around color scheme) as a function of excitation frequency $\omega/2\pi$ and excitation power P. In the lower panel, a vertical slice taken at $\omega/2\pi = 1.375$ GHz (dashed line) shows the abrupt transition between two oscillation states of the system. The upper panel is the result of numerical simulations.

qualitative agreement with the analytical theory which retains only the first anharmonic term in the cosine potential [11]. For instance, the slope of the A-B transition line at the linecut in Fig. 4, $dP\ (\mathrm{dBm})/d\alpha\ (\%) = 0.8$ for the experiment while we calculate its value to be 0.7. Furthermore, in measurements in which the power is ramped in less than 100 ns, we verified that the transition between dynamical states is hysteretic, another prediction of the theory. To explain the complete frequency and power dependence of the transitions shown in the lower panel of Fig. 4, we have performed numerical simulations by solving the full circuit model of the lower corner of Fig. 1, including the exact junction nonlinear constitutive relation. The result of this calculation is shown in the upper panel of Fig. 4. It correctly predicts the variation of the plasma frequency with excitation power, and the boundaries of the phase diffusion region. The agreement between theory and experiment is remarkable in view of the simplicity of the model which uses only measured parameters, and only small differences in the exact shape of region boundaries are observed. It is important to mention that the overall topology of Fig. 4 is unaffected by changes in the parameter values within the bounds of Table I.

In conclusion, we have performed a novel, phase-sensitive, microwave experiment demonstrating that the Josephson plasma oscillation can transition between the two dynamical states predicted for a driven nonlinear system. Using different samples, we have shown that this dynamical phenomenon is stable, reproducible, and can be precisely controlled, thus opening the possibility for practical applications such as amplification. Following the methodology invented for trapped electron systems [12], we can use this dynamical effect as the basis for a single-shot and latching qubit readout.

We thank D. Prober for the use of his laboratory equipment and useful discussions, Abdel Aassime for help in the initial sample fabrication, and L. Grober for assistance with the electron microscope. This work was supported by the ARDA (ARO Grant No. DAAD19-02-1-0044) and by the NSF (Grant No. DMR-0072022).

[1] B. Josephson, Rev. Mod. Phys. **36**, 216 (1964).
[2] B. Yurke, L. R. Corruccini, P. G. Kaminsky, L. W. Rupp, A. D. Smith, A. H. Silver, R. W. Simon, and E. A. Whittaker, Phys. Rev. A **39**, 2519 (1989).
[3] A. J. Dahm, A. Denenstein, T. F. Finnegan, D. N. Langenberg, and D. J. Scalapino, Phys. Rev. Lett. **20**, 859 (1968).
[4] J. Mygind, N. F. Pedersen, and O. H. Soerensen, Appl. Phys. Lett. **29**, 317 (1976).
[5] M. H. Devoret, D. Esteve, J. M. Martinis, A. Cleland, and J. Clarke, Phys. Rev. B **36**, 58 (1987).
[6] T. Holst and J. Bindslev Hansen, Physica (Amsterdam) **165B–166B**, 1649 (1990).
[7] L. D. Landau and E. M. Lifshitz, *Mechanics* (Reed, Oxford, 1981).
[8] T. A. Fulton and L. N. Dunkleberger, Phys. Rev. B **9**, 4760 (1974).
[9] I. Siddiqi, R. Vijay, F. Pierre, C. M. Wilson, M. Metcalfe, C. Rigetti, L. Frunzio, and M. H. Devoret, Phys. Rev. Lett. **93**, 207002 (2004). This work was carried out after the submission of the present Letter.
[10] D. Vion, A. Aassime, A. Cottet, P. Joyez, H. Pothier, C. Urbina, D. Esteve, and M. Devoret, Science **296**, 886 (2002).
[11] M. I. Dykman and V. N. Smelyanski, Phys. Rev. A **41**, 3090 (1990).
[12] C. H. Tseng, D. Enzer, G. Gabrielse, and F. L. Walls, Phys. Rev. A **59**, 2094 (1999).